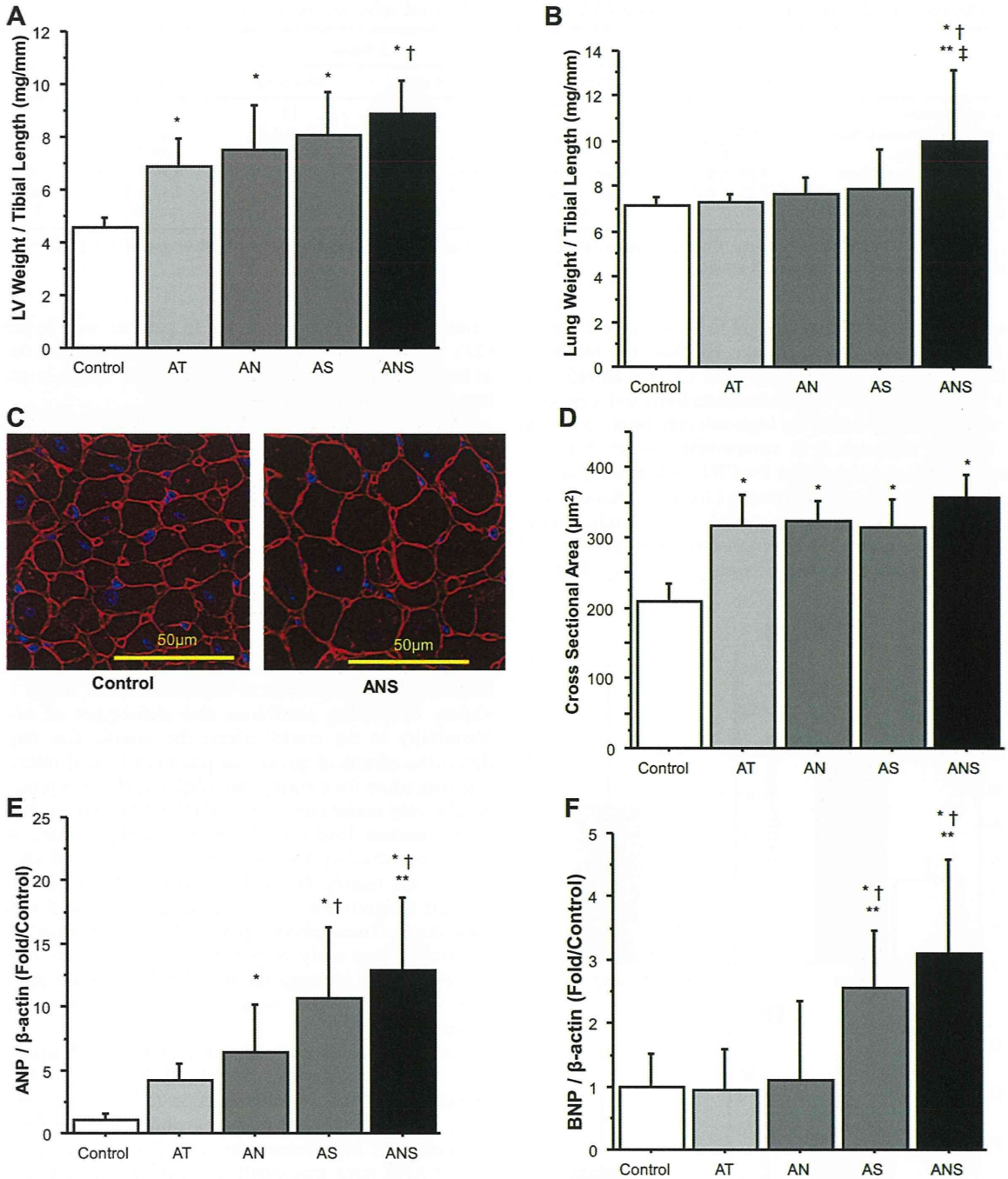

Fig. 3. Organ weights, cross-sectional areas of LV cardiomyocyte, and LV gene expression in the mouse model. *A* and *B*: LV weight/tibial length (*A*) and lung weight/tibial length (*B*) at 6 wk after surgery in control, AT, AN, AS, and ANS mice. *C*: representative examples of lectin-TRITC (red) staining of LV cross-sections. Sections were also stained for nuclei (blue). *D*: values of cross-sectional area of LV cardiomyocytes at 6 wk after the procedures in the five groups. *E* and *F*: atrial natriuretic peptide (ANP; *E*) and brain natriuretic peptide (BNP; *F*) gene expression in the LVs of the five groups. Values are means ± SD. $*P < 0.05$ vs. the control group; $\dagger P < 0.05$ vs. the AT group; $**P < 0.05$ vs. the AN group; $\ddagger P < 0.05$ vs. the AS group.

DISCUSSION

The main finding of this study is that a significant decrease in LV fractional shortening with lung edema was seen after uninephrectomy, high salt intake, and ANG II infusion in this mouse model of HHD. This novel mouse model has several features that mimic clinical HHD (15). Blood pressure was elevated and LV hypertrophy developed at an early stage. Overt HF was observed with cardiac fibrosis, which is considered to be a major determinant of LV dysfunction in HHD (37) at the late stage in this model. ANG II activation is thought to induce hypertension and cardiac hypertrophy, and it also provoked cardiac fibrosis (37). Local activation of the renin-ANG

Table 3. *Physiological parameters of control and ANS mice from 4–6 wk after the procedures*

	4 Weeks		5 Weeks		6 Weeks	
	Control group	ANS group	Control group	ANS group	Control group	ANS group
Number of mice/group	5	5	12	12	12	11
LV end-diastolic dimension, mm	3.5 ± 0.20	3.4 ± 0.24	3.6 ± 0.18	3.5 ± 0.45	3.6 ± 0.24	4.0 ± 0.48*
LV fractional shortening, %	38 ± 5	37 ± 9	42 ± 4	36 ± 6*	39 ± 3	26 ± 9†
LV weight/tibial length, mg/mm	4.35 ± 0.58	6.80 ± 0.69†	4.53 ± 0.40	8.03 ± 1.29†	4.59 ± 0.36	8.90 ± 1.22†
Lung weight/tibial length, mg/mm	7.35 ± 0.71	7.33 ± 0.66	7.47 ± 0.56	9.36 ± 2.77*	7.12 ± 0.40	10.00 ± 3.11†
Mice with congestive heart failure	0	0	0	3 of 12 (25%)	0	7 of 11 (73%)

Results are means ± SD. LV, left ventricular. Congestive heart failure was defined as lung weight/tibial length greater than control +2 ± SD. *$P < 0.05$ vs. the control group; †$P < 0.01$ vs. the control group.

II pathway in the heart is also thought to be one of the crucial factors in the development of chronic HF from the results of many clinical trials and experiments (27). CKD is an independent risk factor in chronic HF. Uninephrectomy induces renal dysfunction, especially under the high-salt condition, in animal models (2, 38), although it is controversial whether uninephrectomy itself is at a risk factor for CKD in humans from the results of patients with cortical tumors (16, 47). Although it is unclear in patients, in the mouse model of this study, uninephrectomy in the presence of hypertension and/or salt loading induced renal dysfunction, which is one of the key determinants in the development of HF in patients with hypertension (27). Thus, the mouse model of the present study is thought to at least partially mimic renal dysfunction, which is one of the key features of HHD in patients.

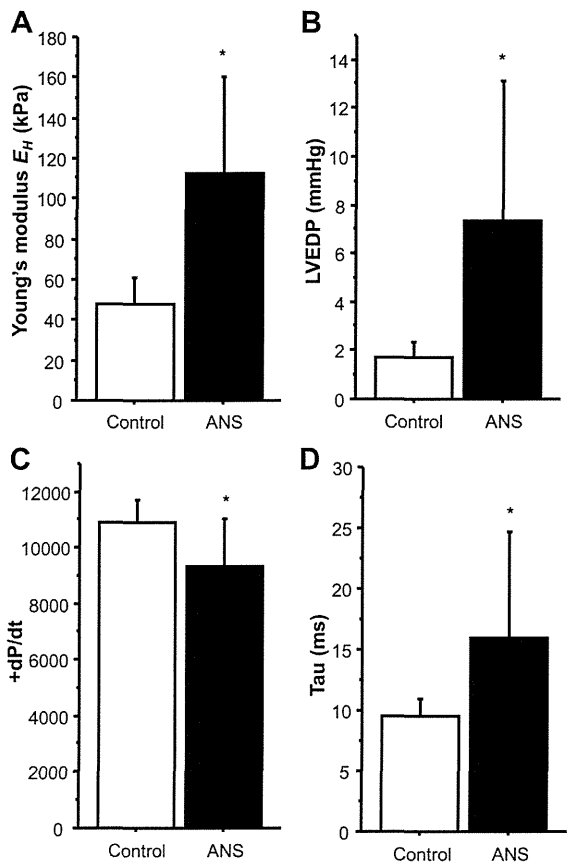

Fig. 4. Myocardial stiffness and hemodynamic parameters. *A*: Young's modulus (E_H), an index of LV myocardial stiffness, in control and ANS mice at 4 wk after surgery. *B–D*: LV end-diastolic pressure (LVEDP; *B*), maximum rate of LV pressure development (+dP/d*t*; *C*), time constant of LV relaxation (τ; *D*) in control and ANS mice at 6 wk after surgery.

Mouse HF models have the great benefit of the wide availability of transgenic or knockout strains of a gene of interest to clarify the pathogenesis of HF and identify novel therapeutic targets (35). The TAC mouse model is a pressure overload model and has been used as a mouse HF model in a number of studies. TAC induces acute significant pressure overload just after the operation and does not necessarily mimic the clinical time course of HHD. Gradual pressure overload models have been reported (43), but it has proven difficult to establish such models in mice. TAC also promotes high mortality, especially just after the operation (26, 28). The performance of TAC in mice requires great surgical expertise, and it might induce a variety of loading conditions and phenotypes of mice (28). Variability in the model affects the sample size required to detect the effects of genetic or pharmacological interventions. The procedure for creating the ANS model in the present study is relatively easier compared with the TAC model, and we can place constant load on each mouse in this model. Approximately one-third of ANS mice died between 3 to 6 wk after the procedures, mainly due to HF, and the rest of the ANS mice showed a significant increase in lung weight at 5–6 wk after procedures. These phenotypes of ANS mice were highly reproducible, and early or perioperative death was rare in this model. Thus, it is suggested that the ANS mouse model has a high incidence of HF with simple and stable experimental procedures.

Previous studies have shown that C57BL/6 mice infused with ANG II show either normal (10, 12, 49) or only minimal impairment in LV systolic function (53) and do not demonstrate HF. In the present study, by adding both high salt intake and unilateral nephrectomy to ANG II infusion, cardiac function of ANS mice was significantly impaired, and mice devel-

Table 4. *Reproducibility of phenotypes of ANS model mice*

	Experiment 1	Experiment 2	Experiment 3
Operated mice	5	5	7
Mortality	1 of 5 (20%)	2 of 5 (40%)	3 of 7 (42%)
Surviving mice	4	3	4
Mice with congestive heart failure	3 of 4 (75%)	2 of 3 (67%)	3 of 4 (75%)
LV weight/tibial length, mg/mm	9.43 ± 1.12	9.01 ± 1.51	8.29 ± 1.14

Results are means ± SD. Congestive heart failure was defined as lung weight/tibial length greater than control +2 ± SD.

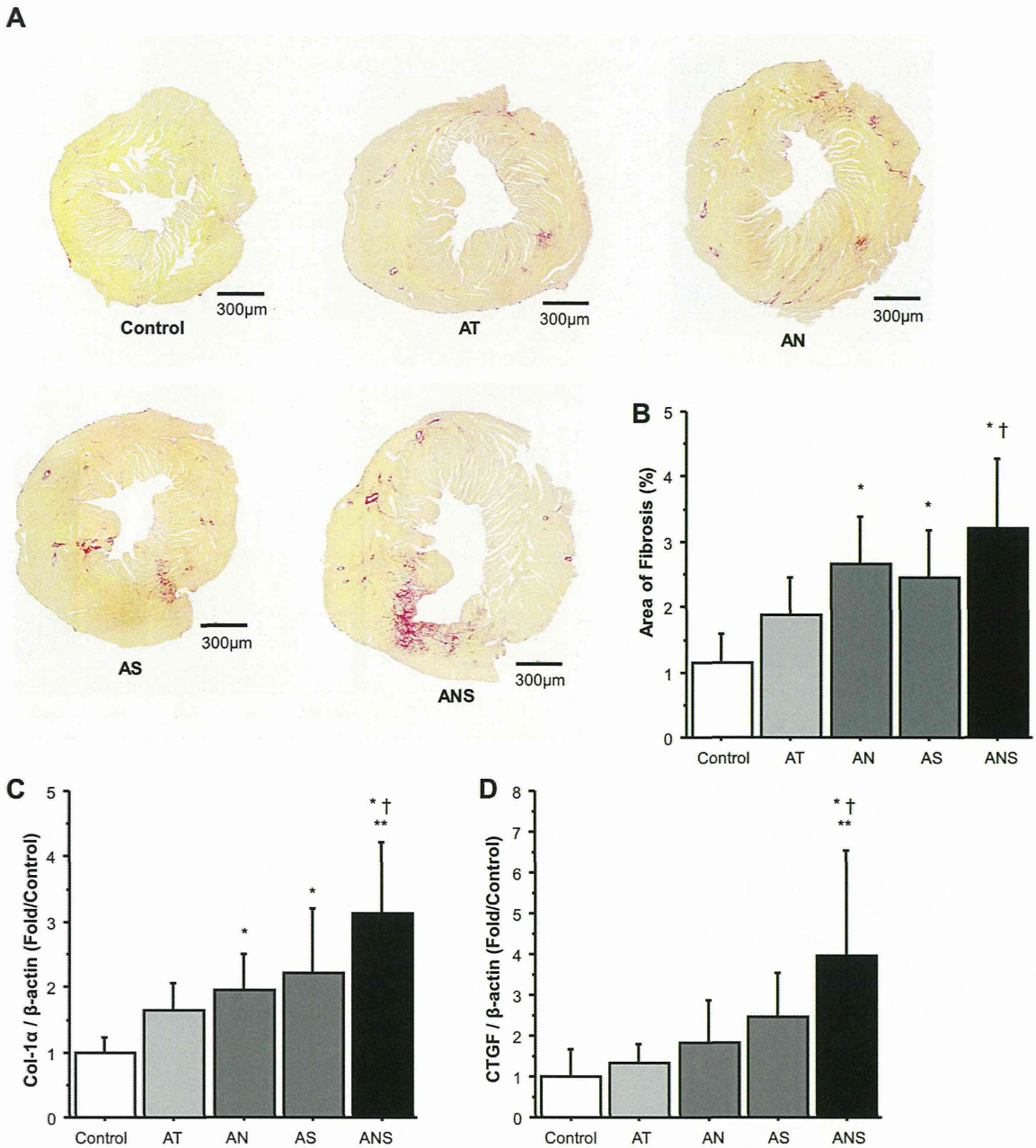

Fig. 5. LV fibrosis in the mouse model. *A*: typical Sirius Red staining of the LV in each group. *B*: percent area of LV fibrosis in control, AT, AN, AS, and ANS mice. *C* and *D*: collagen type 1α (Col-1α; *C*) and connective tissue growth factor (CTGF; *D*) gene expression in the LVs of the five groups. $*P < 0.05$ vs. the control group; $\dagger P < 0.05$ vs. the AT group; $**P < 0.05$ vs. the AN group.

oped HF without a further elevation of blood pressure. Similar cardiomyocyte hypertrophy was seen in the LVs of mice with ANG II infusion irrespective of high salt intake or unilateral nephrectomy. Thus, the enhanced pressure overload and hypertrophy of cardiomyocytes are not considered as the main causes of overt HF in ANS mice.

We preliminary tested the phenotypes in mice with several doses of ANG II infusion, uninephrectomy, and salt loading (data not shown), which demonstrated that 1.2 $mg \cdot kg^{-1} \cdot day^{-1}$ of ANG II infusion is an adequate dose to induce HF in this mouse model of HHD. LV myocardial stiffness increased, LV diastolic and systolic function (as assessed by LV catheterization) was impaired, and LVEDP was elevated with pulmonary edema in ANS mice. LV myocardial stiffening is a major determinant of LV diastolic dysfunction, and it is thought to be provoked by LV fibrosis (51). There might be a mechanism demonstrating that Na^+ and volume overload in the heart with LV diastolic and systolic dysfunction induce overt HF in ANS mice. In the present study, LV ANP mRNA levels increased in AN mice and further increased in ANS mice. LV BNP mRNA

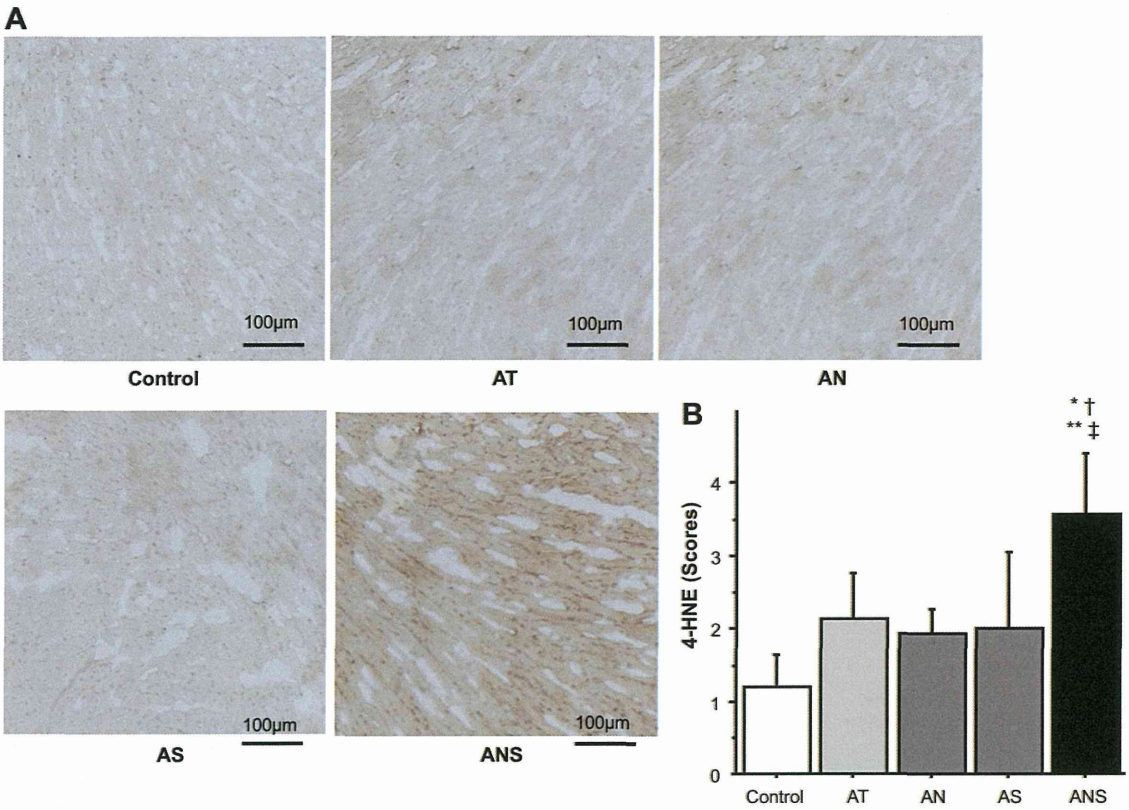

Fig. 6. Oxidative stress in mouse LVs. *A*: typical 4-hydroxy-2-nonenal (4-HNE) staining of the LVs of each group. *B*: scores for semiquantification of 4-HNE staining in the LVs of control, AT, AN, AS, and ANS mice. Values are means ± SD of data from 7–9 mice/group. $*P < 0.05$ vs. the control group; $\dagger P < 0.05$ vs. the AT group; $**P < 0.05$ vs. the AN group; $\ddagger P < 0.05$ vs. the AS group.

levels did not significantly change in AN mice but increased in AS and ANS mice. This suggests that LV ANP expression reflected both cardiac hypertrophy and the salt loading condition, but BNP expression was associated with the salt loading condition and LV fibrosis in our mouse model. These results are consistent with our previous report (39), which showed that ventricular BNP expression was closely related with LV fibrosis in the rat model of diastolic HF. Renal dysfunction has been shown in mice with ANG II infusion and nephrectomy, but overt HF was observed only in ANS mice. When salt intake is increased, Na^+ excretion is promoted, and this increases the glomerular filtration rate and reduces tubular Na^+ reabsorption in normal renal function (18). It has been reported that uninephrectomy does not affect Na^+ excretion under basal conditions but that uninephrectomy induces salt sensitivity and renal injury in the rat model after increased Na^+ intake (2, 38).

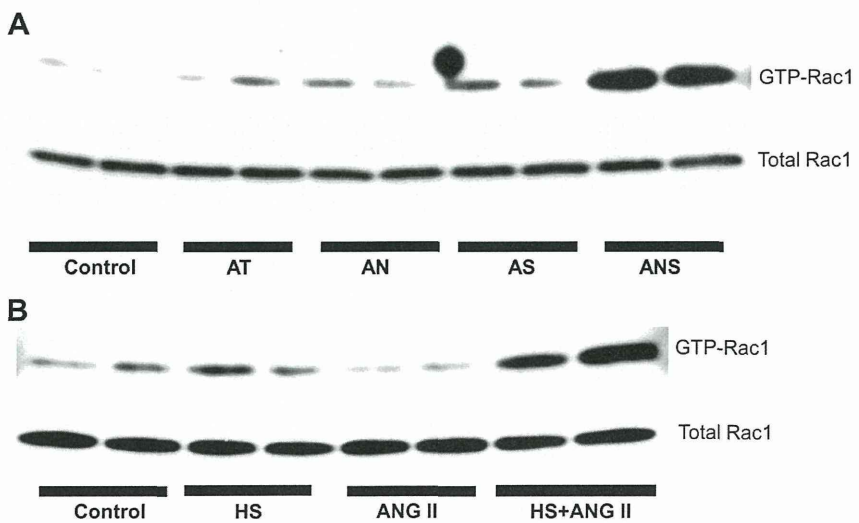

Fig. 7. Rac1 activity in the LVs of the mouse model and cultured cardiomyocytes. *A*: representative Western blots of GTP-bound active Rac1 (GTP-Rac1) and total Rac1 in the LVs of control, AT, AN, AS, and ANS mice. *B*: representative examples of expression of GTP-bound Rac1 and total Rac1 in rat neonatal cardiomyocytes treated with control medium (150 mmol/l Na^+), high-salt (HS) medium (162 mmol/l Na^+), ANG II (1 μmol/l), or both high-salt medium and ANG II for 3 h.

Compensatory mechanisms against Na^+ loading might be insufficient because of renal dysfunction in ANS mice. ANG II can also increase tubular Na^+ reabsorption (22). Thus, ANG II infusion and renal dysfunction induced an impairment of Na^+ homeostasis in ANS mice, and ANS mice are considered to have a tendency toward Na^+ and volume retention. This might be one of the mechanisms that allow ANS mice to demonstrate overt HF. The CKD mouse model induced by 5/6th nephrectomy has also been reported to manifest the HF phenotype, but this has shown conflicting results regarding a cardiac phenotype, such as systolic dysfunction or HF, because the technical instability of 5/6th nephrectomy does not allow the reproduction of similar renal dysfunction in each mouse (20, 23, 24).

It has been reported that Rac1 is activated by high salt loading in the kidney of rodent models of salt-sensitive hypertension and plays a key role in salt sensitivity and salt-induced hypertension (42). Our study suggests that Rac1 activity in cultured cardiomyocytes was increased when cardiomyocytes were in the high Na^+ condition and stimulated with ANG II. In vivo, Rac1 activity was enhanced only in the hearts of ANS mice. It has been reported that Rac1 promotes ROS generation in the heart of the mouse TAC model (3), doxorubicin-induced cardiac toxicity (52), and diabetic cardiomyopathy (41). Previous clinical and experimental studies (1, 14) have provided substantial evidence showing that oxidative stress is enhanced in HF. Excessive ROS production can lead to irreversible cell damage and death in the myocardium, which can impair LV contractile function (8, 48). ROS also stimulate cardiac fibroblast proliferation and activate matrix metalloproteinases, leading to remodeling of the extracellular matrix (40, 48). Rac1 might play a role in LV fibrosis and LV systolic dysfunction through ROS production and contribute to the development of HF in ANS mice.

In conclusion, mice treated with high salt loading, nephrectomy, and ANG II infusion demonstrated a high incidence of HF with simple experimental procedures and reproducible phenotypes. This mouse model will be of interest in investigations of the pathophysiology of HF in HHD and in establishing new options for therapy for HF.

ACKNOWLEDGMENTS

The authors are grateful to Saori Nanbu for the excellent technical assistance in the experiments.

DISCLOSURES

No conflicts of interest, financial or otherwise, are declared by the author(s).

AUTHOR CONTRIBUTIONS

Author contributions: Y. Tsukamoto, T. Mano, Y. Sakata, T.O., Y. Takeda, S.T., Y.O., Y.I., Y. Saito, T. Miwa, K.Y., and I.K. conception and design of research; Y. Tsukamoto, S.T., Y.O., Y.I., Y. Saito, R.I., and M.H. performed experiments; Y. Tsukamoto, T. Mano, Y. Sakata, T.O., Y. Takeda, S.T., Y.O., Y.I., Y. Saito, R.I., M.H., M.K., and T. Miwa analyzed data; Y. Tsukamoto, T. Mano, Y. Sakata, T.O., Y. Takeda, S.T., Y.O., Y.I., Y. Saito, R.I., M.H., M.K., T. Miwa, K.Y., and I.K. interpreted results of experiments; Y. Tsukamoto, T. Mano, and M.K. prepared figures; Y. Tsukamoto, T. Mano, M.H., and M.K. drafted manuscript; Y. Tsukamoto, T. Mano, Y. Sakata, T.O., Y. Takeda, T. Miwa, K.Y., and I.K. edited and revised manuscript; Y. Tsukamoto, T. Mano, Y. Sakata, T.O., Y. Takeda, S.T., Y.O., Y.I., Y. Saito, R.I., M.H., M.K., T. Miwa, K.Y., and I.K. approved final version of manuscript.

REFERENCES

1. **Belch JJ, Bridges AB, Scott N, Chopra M.** Oxygen free radicals and congestive heart failure. *Br Heart J* 65: 245–248, 1991.
2. **Carlstrom M, Sallstrom J, Skott O, Larsson E, Persson AE.** Unilephrectomy in young age or chronic salt loading causes salt-sensitive hypertension in adult rats. *Hypertension* 49: 1342–1350, 2007.
3. **Custodis F, Eberl M, Kilter H, Böhm M, Laufs U.** Association of RhoGDIα with Rac1 GTPase mediates free radical production during myocardial hypertrophy. *Cardiovasc Res* 71: 342–351, 2006.
4. **Doi R, Masuyama T, Yamamoto K, Doi Y, Mano T, Sakata Y, Ono K, Kuzuya T, Hirota S, Koyama T, Miwa T, Hori M.** Development of different phenotypes of hypertensive heart failure: systolic versus diastolic failure in Dahl salt-sensitive rats. *J Hypertens* 18: 111–120, 2000.
5. **Ellmers LJ, Knowles JW, Kim HS, Smithies O, Maeda N, Cameron VA.** Ventricular expression of natriuretic peptides in $Npr1^{-/-}$ mice with cardiac hypertrophy and fibrosis. *Am J Physiol Heart Circ Physiol* 283: H707–H714, 2002.
6. **Go AS, Chertow GM, Fan D, McCulloch CE, Hsu CY.** Chronic kidney disease and the risks of death, cardiovascular events, and hospitalization. *N Engl J Med* 351: 1296–1305, 2004.
7. **Graudal NA, Galløe AM, Garred P.** Effects of sodium restriction on blood pressure, renin, aldosterone, catecholamines, cholesterols, and triglyceride: a meta-analysis. *JAMA* 279: 1383–1391, 1998.
8. **Grieve DJ, Shah AM.** Oxidative stress in heart failure. More than just damage. *Eur Heart J* 24: 2161–2163, 2003.
9. **Gu JW, Anand V, Shek EW, Moore MC, Brady AL, Kelly WC, Adair TH.** Sodium induces hypertrophy of cultured myocardial myoblasts and vascular smooth muscle cells. *Hypertension* 31: 1083–1087, 1998.
10. **Harding P, Yang XP, He Q, Lapointe MC.** Lack of microsomal prostaglandin E synthase-1 reduces cardiac function following angiotensin II infusion. *Am J Physiol Heart Circ Physiol* 300: H1053–H1061, 2011.
11. **Hart CY, Meyer DM, Tazelaar HD, Grande JP, Burnett JC, Housmans PR, Redfield MM.** Load versus humoral activation in the genesis of early hypertensive heart disease. *Circulation* 104: 215–220, 2001.
12. **Haudek SB, Cheng J, Du J, Wang Y, Hermosillo-Rodriguez J, Trial J, Taffet GE, Entman ML.** Monocytic fibroblast precursors mediate fibrosis in angiotensin-II-induced cardiac hypertrophy. *J Mol Cell Cardiol* 49: 499–507, 2010.
13. **Hikoso S, Yamaguchi O, Nakano Y, Takeda T, Omiya S, Mizote I, Taneike M, Oka T, Tamai T, Oyabu J, Uno Y, Matsumura Y, Nishida K, Suzuki K, Kogo M, Hori M, Otsu K.** The IκB kinase β/nuclear factor κB signaling pathway protects the heart from hemodynamic stress mediated by the regulation of manganese superoxide dismutase expression. *Circ Res* 105: 70–79, 2009.
14. **Hill MF, Singal PK.** Antioxidant and oxidative stress changes during heart failure subsequent to myocardial infarction in rats. *Am J Pathol* 148: 291–300, 1996.
15. **Houser SR, Margulies KB, Murphy AM, Spinale FG, Francis GS, Prabhu SD, Rockman HA, Kass DA, Molkentin JD, Sussman MA, Koch WJ, Koch W; American Heart Association Council on Basic Cardiovascular Sciences, Council on Clinical Cardiology, Council on Functional Genomics and Translational Biology.** Animal models of heart failure: a scientific statement from the American Heart Association. *Circ Res* 111: 131–150, 2012.
16. **Huang WC, Levey AS, Serio AM, Snyder M, Vickers AJ, Raj GV, Scardino PT, Russo P.** Chronic kidney disease after nephrectomy in patients with renal cortical tumours: a retrospective cohort study. *Lancet Oncol* 7: 735–740, 2006.
17. **Ishii R, Higashimori M, Tadakuma K, Kaneko M, Tamaki S, Sakata Y, Yamamoto K.** Balloon type elasticity sensing for left ventricle of small laboratory animal. *Conf Proc IEEE Eng Med Biol Soc* 2011: 904–907, 2011.
18. **Ito S, Nagasawa T, Abe M, Mori T.** Strain vessel hypothesis: a viewpoint for linkage of albuminuria and cerebro-cardiovascular risk. *Hypertens Res* 32: 115–121, 2009.
19. **Kakoki M, Kizer CM, Yi X, Takahashi N, Kim HS, Bagnell CR, Edgell CJ, Maeda N, Jennette JC, Smithies O.** Senescence-associated phenotypes in Akita diabetic mice are enhanced by absence of bradykinin B_2 receptors. *J Clin Invest* 116: 1302–1309, 2006.
20. **Kennedy DJ, Elkareh J, Shidyak A, Shapiro AP, Smaili S, Mutgi K, Gupta S, Tian J, Morgan E, Khouri S, Cooper CJ, Periyasamy SM, Xie Z, Malhotra D, Fedorova OV, Bagrov AY, Shapiro JI.** Partial nephrectomy as a model for uremic cardiomyopathy in the mouse. *Am J Physiol Renal Physiol* 294: F450–F454, 2008.
21. **Keppler A, Gretz N, Schmidt R, Kloetzer HM, Groene HJ, Lelongt B, Meyer M, Sadick M, Pill J.** Plasma creatinine determination in mice and

rats: an enzymatic method compares favorably with a high-performance liquid chromatography assay. *Kidney Int* 71: 74–78, 2007.

22. **Kopkan L, Cervenka L.** Renal interactions of renin-angiotensin system, nitric oxide and superoxide anion: implications in the pathophysiology of salt-sensitivity and hypertension. *Physiol Res* 58, *Suppl* 2: S55–S67, 2009.
23. **Leelahavanichkul A, Yan Q, Hu X, Eisner C, Huang Y, Chen R, Mizel D, Zhou H, Wright EC, Kopp JB, Schnermann J, Yuen PS, Star RA.** Angiotensin II overcomes strain-dependent resistance of rapid CKD progression in a new remnant kidney mouse model. *Kidney Int* 78: 1136–1153, 2010.
24. **Li Y, Takemura G, Okada H, Miyata S, Maruyama R, Esaki M, Kanamori H, Li L, Ogino A, Ohno T, Kondo T, Nakagawa M, Minatoguchi S, Fujiwara T, Fujiwara H.** Molecular signaling mediated by angiotensin II type 1A receptor blockade leading to attenuation of renal dysfunction-associated heart failure. *J Card Fail* 13: 155–162, 2007.
25. **Liao CH, Akazawa H, Tamagawa M, Ito K, Yasuda N, Kudo Y, Yamamoto R, Ozasa Y, Fujimoto M, Wang P, Nakauchi H, Nakaya H, Komuro I.** Cardiac mast cells cause atrial fibrillation through PDGF-A-mediated fibrosis in pressure-overloaded mouse hearts. *J Clin Invest* 120: 242–253, 2010.
26. **Liao Y, Ishikura F, Beppu S, Asakura M, Takashima S, Asanuma H, Sanada S, Kim J, Ogita H, Kuzuya T, Node K, Kitakaze M, Hori M.** Echocardiographic assessment of LV hypertrophy and function in aortic-banded mice: necropsy validation. *Am J Physiol Heart Circ Physiol* 282: H1703–H1708, 2002.
27. **Luque M, de Rivas B, Divison JA, Marquez E, Sobreviela E.** Relationship between renal function and heart failure in hypertensive patients. *Intern Med J* 40: 76–79, 2010.
28. **Mohammed SF, Storlie JR, Oehler EA, Bowen LA, Korinek J, Lam CS, Simari RD, Burnett JC Jr, Redfield MM.** Variable phenotype in murine transverse aortic constriction. *Cardiovasc Pathol* 21: 188–198, 2012.
29. **Ohtani T, Mano T, Hikoso S, Sakata Y, Nishio M, Takeda Y, Otsu K, Miwa T, Masuyama T, Hori M, Yamamoto K.** Cardiac steroidogenesis and glucocorticoid in the development of cardiac hypertrophy during the progression to heart failure. *J Hypertens* 27: 1074–1083, 2009.
30. **Ohtani T, Ohta M, Yamamoto K, Mano T, Sakata Y, Nishio M, Takeda Y, Yoshida J, Miwa T, Okamoto M, Masuyama T, Nonaka Y, Hori M.** Elevated cardiac tissue level of aldosterone and mineralocorticoid receptor in diastolic heart failure: beneficial effects of mineralocorticoid receptor blocker. *Am J Physiol Regul Integr Comp Physiol* 292: R946–R954, 2007.
31. **Oka T, Maillet M, Watt AJ, Schwartz RJ, Aronow BJ, Duncan SA, Molkentin JD.** Cardiac-specific deletion of Gata4 reveals its requirement for hypertrophy, compensation, and myocyte viability. *Circ Res* 98: 837–845, 2006.
32. **Omiya S, Hikoso S, Imanishi Y, Saito A, Yamaguchi O, Takeda T, Mizote I, Oka T, Taneike M, Nakano Y, Matsumura Y, Nishida K, Sawa Y, Hori M, Otsu K.** Downregulation of ferritin heavy chain increases labile iron pool, oxidative stress and cell death in cardiomyocytes. *J Mol Cell Cardiol* 46: 59–66, 2009.
33. **Omori Y, Ohtani T, Sakata Y, Mano T, Takeda Y, Tamaki S, Tsukamoto Y, Kamimura D, Aizawa Y, Miwa T, Komuro I, Soga T, Yamamoto K.** L-Carnitine prevents the development of ventricular fibrosis and heart failure with preserved ejection fraction in hypertensive heart disease. *J Hypertens* 30: 1834–1844, 2012.
34. **Pacher P, Nagayama T, Mukhopadhyay P, Bátkai S, Kass DA.** Measurement of cardiac function using pressure-volume conductance catheter technique in mice and rats. *Nat Protoc* 3: 1422–1434, 2008.
35. **Patten RD, Hall-Porter MR.** Small animal models of heart failure: development of novel therapies, past and present. *Circ Heart Fail* 2: 138–144, 2009.
36. **Pfeffer JM, Pfeffer MA, Mirsky I, Braunwald E.** Regression of left ventricular hypertrophy and prevention of left ventricular dysfunction by captopril in the spontaneously hypertensive rat. *Proc Natl Acad Sci USA* 79: 3310–3314, 1982.
37. **Querejeta R, Lopez B, Gonzalez A, Sanchez E, Larman M, Martinez Ubago JL, Diez J.** Increased collagen type I synthesis in patients with heart failure of hypertensive origin: relation to myocardial fibrosis. *Circulation* 110: 1263–1268, 2004.
38. **Rodriguez-Gomez I, Wangensteen R, Perez-Abud R, Quesada A, Del Moral RG, Osuna A, O'Valle F, de Dios Luna J, Vargas F.** Long-term consequences of uninephrectomy in male and female rats. *Hypertension* 60: 1458–1463, 2012.
39. **Sakata Y, Yamamoto K, Masuyama T, Mano T, Nishikawa N, Kuzuya T, Miwa T, Hori M.** Ventricular production of natriuretic peptides and ventricular structural remodeling in hypertensive heart failure. *J Hypertens* 19: 1905–1912, 2001.
40. **Segura AM, Frazier OH, Buja LM.** Fibrosis and heart failure. *Heart Fail Rev.* In press.
41. **Shen E, Li Y, Shan L, Zhu H, Feng Q, Arnold JM, Peng T.** Rac1 is required for cardiomyocyte apoptosis during hyperglycemia. *Diabetes* 58: 2386–2395, 2009.
42. **Shibata S, Mu S, Kawarazaki H, Muraoka K, Ishizawa K, Yoshida S, Kawarazaki W, Takeuchi M, Ayuzawa N, Miyoshi J, Takai Y, Ishikawa A, Shimosawa T, Ando K, Nagase M, Fujita T.** Rac1 GTPase in rodent kidneys is essential for salt-sensitive hypertension via a mineralocorticoid receptor-dependent pathway. *J Clin Invest* 121: 3233–3243, 2011.
43. **Siri FM, Nordin C, Factor SM, Sonnenblick E, Aronson R.** Compensatory hypertrophy and failure in gradual pressure-overloaded guinea pig heart. *Am J Physiol Heart Circ Physiol* 257: H1016–H1024, 1989.
44. **Strazzullo P, D'Elia L, Kandala NB, Cappuccio FP.** Salt intake, stroke, and cardiovascular disease: meta-analysis of prospective studies. *BMJ* 339: b4567, 2009.
45. **Tamaki S, Mano T, Sakata Y, Ohtani T, Takeda Y, Kamimura D, Omori Y, Tsukamoto Y, Ikeya Y, Kawai M, Kumanogoh A, Hagihara K, Ishii R, Higashimori M, Kaneko M, Hasuwa H, Miwa T, Yamamoto K, Komuro I.** Interleukin-16 promotes cardiac fibrosis and myocardial stiffening in heart failure with preserved ejection fraction. *PLos One* 8: e68893, 2013.
46. **Terui T, Shimamoto Y, Yamane M, Kobirumaki F, Ohtsuki I, Ishiwata S, Kurihara S, Fukuda N.** Regulatory mechanism of length-dependent activation in skinned porcine ventricular muscle: role of thin filament cooperative activation in the Frank-Starling relation. *J Gen Physiol* 136: 469–482, 2010.
47. **Torricelli FC, Danilovic A, Marchini GS, Sant'Anna AC, Dall'Oglio MF, Srougi M.** Can we predict which patients will evolve to chronic kidney disease after nephrectomy for cortical renal tumors? *Int Braz J Urol* 38: 637–644, 2012.
48. **Tsutsui H, Kinugawa S, Matsushima S.** Oxidative stress and heart failure. *Am J Physiol Heart Circ Physiol* 301: H2181–H2190, 2011.
49. **Xu Z, Okamoto H, Akino M, Onozuka H, Matsui Y, Tsutsui H.** Pravastatin attenuates left ventricular remodeling and diastolic dysfunction in angiotensin II-induced hypertensive mice. *J Cardiovasc Pharmacol* 51: 62–70, 2008.
50. **Yamamoto K, Masuyama T, Sakata Y, Doi R, Ono K, Mano T, Kondo H, Kuzuya T, Miwa T, Hori M.** Local neurohumoral regulation in the transition to isolated diastolic heart failure in hypertensive heart disease: absence of AT_1 receptor downregulation and 'overdrive' of the endothelin system. *Cardiovasc Res* 46: 421–432, 2000.
51. **Yamamoto K, Masuyama T, Sakata Y, Nishikawa N, Mano T, Yoshida J, Miwa T, Sugawara M, Yamaguchi Y, Ookawara T, Suzuki K, Hori M.** Myocardial stiffness is determined by ventricular fibrosis, but not by compensatory or excessive hypertrophy in hypertensive heart. *Cardiovasc Res* 55: 76–82, 2002.
52. **Yoshida M, Shiojima I, Ikeda H, Komuro I.** Chronic doxorubicin cardiotoxicity is mediated by oxidative DNA damage-ATM-p53-apoptosis pathway and attenuated by pitavastatin through the inhibition of Rac1 activity. *J Mol Cell Cardiol* 47: 698–705, 2009.
53. **Zhang R, Zhang YY, Huang XR, Wu Y, Chung AC, Wu EX, Szalai AJ, Wong BC, Lau CP, Lan HY.** C-reactive protein promotes cardiac fibrosis and inflammation in angiotensin II-induced hypertensive cardiac disease. *Hypertension* 55: 953–960, 2010.

Cardiovasc Drugs Ther (2013) 27:125–132
DOI 10.1007/s10557-012-6437-6

ORIGINAL ARTICLE

Liposomal Amiodarone Augments Anti-arrhythmic Effects and Reduces Hemodynamic Adverse Effects in an Ischemia/Reperfusion Rat Model

Hiroyuki Takahama · Hirokazu Shigematsu · Tomohiro Asai · Takashi Matsuzaki · Shoji Sanada · Hai Ying Fu · Keiji Okuda · Masaki Yamato · Hiroshi Asanuma · Yoshihiro Asano · Masanori Asakura · Naoto Oku · Issei Komuro · Masafumi Kitakaze · Tetsuo Minamino

Published online: 24 January 2013

Abstract
Purpose Although amiodarone is recognized as the most effective anti-arrhythmic drug available, it has negative hemodynamic effects. Nano-sized liposomes can accumulate in and selectively deliver drugs to ischemic/reperfused (I/R) myocardium, which may augment drug effects and reduce side effects. We investigated the effects of liposomal amiodarone on lethal arrhythmias and hemodynamic parameters in an ischemia/reperfusion rat model.
Methods and Results We prepared liposomal amiodarone (mean diameter: 113±8 nm) by a thin-film method. The left coronary artery of experimental rats was occluded for 5 min followed by reperfusion. Ex vivo fluorescent imaging revealed that intravenously administered fluorescent-labeled nano-sized beads accumulated in the I/R myocardium. Amiodarone was measurable in samples from the I/R myocardium when liposomal amiodarone, but not amiodarone, was administered. Although the intravenous administration of amiodarone (3 mg/kg) or liposomal amiodarone (3 mg/kg) reduced heart rate and systolic blood pressure compared with saline, the decrease in heart rate or systolic blood pressure caused by liposomal amiodarone was smaller compared with a corresponding dose of free amiodarone. The intravenous administration of liposomal amiodarone (3 mg/kg), but not free amiodarone (3 mg/kg), 5 min before ischemia showed a significantly reduced duration of lethal arrhythmias (18±9 s) and mortality (0 %) during the reperfusion period compared with saline (195±42 s, 71 %, respectively).
Conclusions Targeting the delivery of liposomal amiodarone to ischemic/reperfused myocardium reduces the mortality due to lethal arrhythmia and the negative hemodynamic changes caused by amiodarone. Nano-size liposomes may be a promising drug delivery system for targeting I/R myocardium with cardioprotective agents.

Keywords Liposome · Amiodarone · Lethal arrhythmia · Ischemia · Reperfusion

T. Matsuzaki · S. Sanada · H. Y. Fu · K. Okuda · M. Yamato · Y. Asano · I. Komuro · T. Minamino (✉)
Department of Cardiovascular Medicine, Osaka University Graduate School of Medicine, 2-2 Yamadaoka, Suita, Osaka 565-0871, Japan
e-mail: minamino@cardiology.med.osaka-u.ac.jp

H. Takahama · M. Asakura · M. Kitakaze
Department of Cardiovascular Medicine, National Cerebral and Cardiovascular Center, Suita 565-8565, Japan

H. Shigematsu · T. Asai · N. Oku
Department of Medical Biochemistry and Global COE, University of Shizuoka Graduate School of Pharmaceutical Sciences, Shizuoka 422-8526 Shizuoka, Japan

H. Asanuma
Department of Cardiovascular Science and Technology, Kyoto Prefectural University School of Medicine, Kyoto 602-8566, Japan

H. Takahama
Division of Cardiovascular Disease, Mayo Clinic, Rochester, MN 55902, USA

Introduction

Therapies for the prevention and treatment of ischemia-induced life-threatening arrhythmias remain an unmet medical need [1]. Amiodarone is currently considered to be the most effective anti-arrhythmic drug available for treating life-threatening arrhythmias [2, 3], despite the fact that this compound has a negative impact on hemodynamic parameters [4, 5]. The intravenous administration of amiodarone is expected

to be beneficial for the immediate treatment of arrhythmias in emergency settings, such as acute myocardial infarction (AMI) [6, 7]. However, in clinical practice, the administration of amiodarone remains problematic for the treatment of AMI [8]. Although lower doses of amiodarone result in fewer incidences of death, high doses of amiodarone can cause hypotension and non-cardiac death, both of which may diminish the positive effects of amiodarone [8, 9]. Therefore, a novel delivery system is strongly desired to enhance the anti-arrhythmic effects of amiodarone without producing severe side effects.

Liposomes are widely used for drug delivery to actively or passively target specific organs and to improve drug stability in cancer and inflammatory diseases [10–12]. In ischemic/reperfused (I/R) myocardium, cellular permeability is enhanced and vascular endothelial integrity is disrupted [13, 14], suggesting that nanoparticles, such as liposomes, may be a promising drug delivery system for targeting I/R myocardium with cardioprotective agents [15]. Indeed, we have recently demonstrated that adenosine encapsulated by liposomes coated with polyethylene glycol (PEG) exhibited enhanced cardioprotective effects and attenuated side effects, such as hypotension and bradycardia, in an ischemia/reperfusion model of rats [16]. In the present study, we prepared liposomal amiodarone and examined 1) the targeted accumulation of liposomal amiodarone in the I/R myocardium, 2) the hemodynamic effects of the intravenous administration of liposomal amiodarone and free amiodarone, and 3) the anti-arrhythmic effects of these preparations in an I/R rat model. We showed that targeting the delivery of liposomal amiodarone to I/R myocardium reduces the mortality due to lethal arrhythmias and the negative hemodynamic changes caused by amiodarone in an I/R rat model.

Methods

Materials

The materials used to prepare PEGylated liposomes, including 1-palmitoyl-2-oleoyl-sn-glycero-3-phosphocholine (POPC), 1,2-dipalmitoyl-sn-glycero-3-phosphocholine (DPPC), cholesterol, and 1,2-distearoyl-sn-glycero-3-phosphoethanolamine-N-poly(ethylene glycol) 2000 (DSPE-PEG2000), were kindly donated by Nippon Fine Chemical Co. (Takasago, Hyogo, Japan). Fluorescent beads (diameter 100 nm) were purchased from Invitrogen. All other materials were obtained from Sigma-Aldrich (St. Louis, MO, USA).

Animals

Male Wistar rats (9 weeks old and weighing 250–310 g; Japan Animals, Osaka, Japan) were used. The animal experiments were approved by the Osaka University Research Committee and were performed according to institutional guidelines. All studies conformed to the Guide for the care and Use of Laboratory Animals published by the US National Institutes of Health (NIH Publication No. 85–23, revised 1996).

Preparation of PEGylated Liposomes

PEGylated liposomes composed of POPC, DPPC, cholesterol, DSPE-PEG2000, and amiodarone were prepared by a thin-film method. Briefly, amiodarone and lipids dissolved in chloroform were evaporated to form a thin lipid film using a rotary evaporator. The lipid film was dried for at least 1 h under reduced pressure and then hydrated with PBS (pH7.4). The liposome solution was freeze-thawed for 3 cycles with liquid nitrogen. The particle size of the liposomes was adjusted by extrusion through 100-nm-pore polycarbonate filters (Nuclepore, Cambridge, MA, USA). The liposomal solutions were centrifuged at 453,000 g for 15 min (CS120GXL, Hitachi, Japan) to remove the untrapped amiodarone. Then, the liposomes were resuspended in PBS. To determine the efficacy of trapping amiodarone in the liposomes, an aliquot of the liposomal solution was solubilized with 1 % reduced Triton X-100 (Sigma-Aldrich), and the amount of amiodarone was optically determined at 240 nm.

Characterization of PEGylated Liposomes

The particle size and ζ potential of PEGylated liposomes diluted with PBS were measured by dynamic scatter analysis (Zetasizer Nano ZS; Malvern, Worcestershire, UK). The analyses were performed 15 times per sample, and the results represent the analysis of 3 independent experiments.

Experimental Protocol

Targeted Delivery of Fluorescent-labeled Nano-sized Beads to the I/R Myocardium

The rats were anesthetized with intraperitoneal sodium pentobarbital (50 mg/kg). Catheters were advanced into the femoral vein to infuse the drugs. Ischemia/reperfusion was induced by 5 min of left coronary artery occlusion followed by reperfusion [16]. After the hemodynamic parameters became stable, fluorescent-labeled nano-size beads, 100 nm in diameter (FluoSpheres, Invitrogen), were intravenously infused to the rats for 5 min before ischemia or before a sham operation (n=3, each). Fifteen minutes after reperfusion, the hearts were removed and cut into 5 sections parallel to the axis from the base to the apex. Then, ex vivo fluorescence images were obtained with an Olympus SZX12 stereoscopic microscope equipped with a DP71 digital camera (Olympus, Tokyo, Japan) before and after the hearts were sliced.

Targeted Delivery of Amiodarone and Liposomal Amiodarone to the I/R Myocardium

Catheters were advanced into the femoral artery and vein to measure the systemic blood pressure (BP) and to infuse the drugs into the anesthetized rats, respectively. Electrocardiographic and hemodynamic parameters, such as heart rate (HR) and BP, were continuously monitored during the study using a PowerLab system (ADInstruments, Castle Hill, Australia). After the hemodynamic parameters became stable, to clarify the targeted delivery of amiodarone and liposomal amiodarone to the I/R myocardium, we intravenously administered saline, free amiodarone (3 mg/kg) or liposomal amiodarone (3 mg/kg) to rats for 5 min before the onset of ischemia. Then, we obtained blood samples and myocardium from the I/R area.

Effects of Amiodarone and Liposomal Amiodarone on Lethal Arrhythmias

To evaluate the effects of amiodarone and liposomal amiodarone on lethal arrhythmias, we intravenously administered saline (n=7), free amiodarone (3.0 or 10.0 mg/kg) (n=6 each), PEGylated liposomes (empty liposomes) (n=6), and PEGylated liposomal amiodarone (3.0 mg/kg) (n=6) for 5 min before ischemia. The dose of amiodarone used in this study was lower than that used in a previous study [17] to clarify whether amiodarone encapsulated by liposomes coated with PEG exhibited enhanced anti-arrhythmic effects. Without any procedure such as electrical conversion or cardiac massage, ventricular tachyarrhythmias (VT/VF) occurred frequently during early period of reperfusion and the mortality of rats reached more than a half of cases in this model [18].

Measurement of Amiodarone Concentration

The concentration of amiodarone in serum and heart tissue from the I/R area was assayed by high-performance liquid chromatography (HPLC) as previously described [19]. The detection limit of the HPLC assay was 50 ng/mL. Blood and myocardial samples were obtained at the end of the experimental protocol. The sample preparation was performed as previously described [19]. Briefly, myocardium was freed from visible blood, thereafter rinsed with 0.9 % sodium chloride and stored at −20 °C until analysis. After that, myocardial tissue samples were finely minced and 100 mg were homogenized with 0.9 % sodium chloride (1 mL) and after centrifugation, the clear supernatant was injected into HPLC.

Quantitative Evaluation of Fluorescent-labeled Nano-sized Beads in the I/R Myocardium

To analyze the quantitative fluorescent intensity, signals from heart slices were quantified by image analysis (Image J; National Institutes of Health, USA) as previously described [20]. The signal intensity from the heart slices was evaluated as the average signals of the whole heart and the left ventricle (LV) (Fig. 2c).

Arrhythmia Analysis

The electrocardiographic tracings were independently analyzed by two of the authors, who were blinded to the treatment assignment. The duration of each spontaneous ventricular tachycardia or fibrillation episode during the I/R protocol was measured using the time scale provided by the recording software. Ventricular tachycardia was defined as 4 or more consecutive ventricular ectopic beats, and ventricular fibrillation was defined as a signal in which the individual QRS deflections could not easily be distinguished from one another. However, distinguishing ventricular tachycardia from fibrillation was often difficult [21]; therefore, we report ventricular tachycardia and fibrillation collectively as ventricular tachyarrhythmias (VT/VF) in this study. VT/VF duration and mortality were evaluated for 5 min of ischemia followed by 15 min of reperfusion.

Statistical Analysis

The parameters of the liposomes are expressed as the mean ± standard deviation (SD). Other data are expressed as the average ± standard error of the mean (SEM). To compare the parameters of the liposomes, unpaired t-tests were performed. We performed the Welch t-test to compare the amiodarone concentration in the plasma and myocardium. For hemodynamic parameters, the data were assessed with the paired t-test for comparisons to the baseline within a group. One-way repeated-measurement ANOVA followed by post-hoc Bonferroni's multiple comparisons were used for comparisons between groups. To address the differences in VT/VF duration among the groups, we performed a non-parametric (Kruskal-Wallis) test followed by evaluation with the Mann–Whitney U test. The mortality rates were compared using the Fisher's exact probability test. In all analyses, $P<0.05$ was considered to be statistically significant.

Results

Characterization of PEGylated Liposomes

We prepared 5 types of PEGylated liposomes composed of POPC, DPPC, cholesterol, and amiodarone. The ratio of unsaturated lipids (POPC) to saturated lipids (DPPC) varied (Fig. 1). During preparation of the liposomes, the POPC:DPPC:cholesterol:amiodarone molar ratio of 10:0:5:1 exhibited the best encapsulation efficiency for amiodarone compared with the other conditions (Fig. 1).

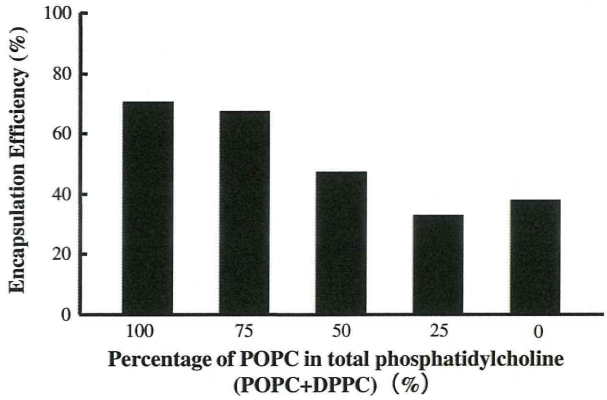

Fig. 1 Encapsulation efficiency of amiodarone in the liposomes. Amiodarone was loaded into liposomes containing POPC, DPPC, or a mixture of POPC and DPPC. The liposomal amiodarone was composed of phosphatidylcholine (POPC + DPPC):cholesterol:amiodarone at a 10:5:1 molar ratio. The percent molar ratio of POPC in total phosphatidylcholine (POPC + DPPC) is indicated in the figure. The encapsulation efficiency of amiodarone was determined as described in the Methods section

The dynamic light scatter analysis showed no significant differences between the mean diameter, polydispersity index, or ζ potential distribution of the empty and amiodarone-loaded PEGylated liposomes (Table 1).

Accumulation of Fluorescence-labeled Nano-sized Beads in the I/R Myocardium

Representative pictures obtained by fluorescence imaging are shown in Fig. 2a (whole heart) and b (sliced hearts). Quantitative analysis revealed that the average fluorescence intensity of the whole heart (Fig. 2c left) or the left ventricle (Fig. 2c right) of the I/R hearts was significantly higher than that in sham-operated hearts.

Amiodarone Concentration in the Blood and I/R Myocardium

The plasma concentration after the administration of liposomal amiodarone was significantly higher than that of free amiodarone (Table 2). Importantly, the amiodarone concentration in the I/R myocardium was detectable after the administration of liposomal, but not free, amiodarone (Table 2).

Hemodynamic Effects of Amiodarone and Liposomal Amiodarone

The baseline heart rates were 411±16, 426±14, 427±12, 409±8 and 414±6 beats/min in the saline, empty liposome, amiodarone (3 mg/kg), amiodarone (10 mg/kg) and liposomal amiodarone (3 mg/kg) groups, respectively. The baseline systolic BP was 113±7, 118±10, 111±5, 90±4 and 104±2 mmHg in the saline, empty liposome, amiodarone (3 mg/kg), amiodarone (10 mg/kg) and liposomal amiodarone (3 mg/kg) groups, respectively. There were no significant differences in the baseline HR or systolic BP among the groups tested. The intravenous administration of amiodarone (3 and 10 mg/kg) or liposomal amiodarone reduced both the HR and systolic BP from the baseline, whereas the saline or empty liposomes did not (Fig. 3). The time-course changes of both the HR and systolic BP were significantly smaller in the liposomal amiodarone group (3 mg/kg) compared with the corresponding dose in the free amiodarone group (3 mg/kg) (Fig. 3). The reductions in HR and systolic BP at 1, but not 3, minutes after liposomal amiodarone administration were significantly smaller compared with those following the corresponding dose of amiodarone.

Antiarrhythmic Effects of Amiodarone and Liposomal Amiodarone

Representative electrocardiograms of the rats that received saline, free amiodarone or liposomal amiodarone are shown in Fig. 4. The intravenous administration of liposomal amiodarone (3 mg/kg), but not amiodarone (3 mg/kg), significantly reduced the duration of VT/VF compared with saline (Table 3). Furthermore, the mortality in the group that received liposomal amiodarone (3 mg/kg), but not the corresponding dose of amiodarone (3 mg/kg), was significantly lower than that in the saline group. In the group of rats that received a high dose of amiodarone (10 mg/kg), the VT/VF duration was 36±12 s, and none of the rats died (Table 3), which was similar to the low dose of liposomal amiodarone group (3 mg/kg).

Discussion

In this study, we revealed that 1) liposomal amiodarone was successfully prepared using a thin-film method, 2) the

Table 1 Characterization of liposomes by dynamic light scatter analysis

	Mean diameter (nm)	Polydispersity index	ζ Potential (mV)
PEGylated liposomes (empty liposomes)	111±14	0.124±0.027	−2.1
PEGylated liposomal amiodarone	113±8	0.128±0.040	−3.7

Results represent 4 independent experiments. The values are expressed as the mean ± SD. *PEG* polyethylene glycol